journal

Microstructures and Positron Annihilation Spectroscopy of Nearly Stoichiometric ZrC Coating Layers for Advanced High-temperature Gas-Cooled Reactor Fuel

Jun Aihara,[‡,†] Masaki Maekawa,[§] Shohei Ueta,[‡] Atsuo Kawasuso,[§] and Kazuhiro Sawa[‡]

[‡]Oarai Research and Development Center, Japan Atomic Energy Agency, Ibaraki-ken, Japan

[§]Advanced Science Research Center, Japan Atomic Energy Agency, Takasaki, Gunma, Japan

The Japan Atomic Energy Agency (JAEA) has started to study and develop zirconium carbide (ZrC)-coated fuel particles for advanced high-temperature gas-cooled reactors. The ZrC-coated particles have been fabricated at JAEA and then heat-treated to investigate the effects of the fuel compact sintering process. Remarkable ZrC crystal grain growth occurred in one batch, but not in another, in spite of both having the same C/Zr ratio and ZrC density. TEM/STEM observation of the specimens before heat treatment clarified that considerably more free carbons or voids, which would be expected to hinder the grain growth of ZrC with heat treatment, were distributed in the ZrC layer in the batch in which the remarkable ZrC crystal grain growth did not occur than in the other batch. Differences between these batches, which could not be detected by estimating the C/Zr ratio or the ZrC density, could be detected with positron annihilation spectroscopy (PAS). This result indicates that there is a possibility that PAS can be applied for quality control for ZrC-coated fuel particles in the future, as preparing specimens for PAS is much easier than for TEM/STEM observation. Moreover, PAS is much more suitable than microstructural observation for quantitative estimation. Characterization of defects detected with PAS would be the next step in this process for the investigation of the feasibility of the application of PAS to the quality control of ZrC-coated fuel particles.

I. Introduction

$\mathbf{T}$HE high-temperature gas-cooled reactor (HTGR) is a type of nuclear reactor that utilizes ceramic-coated UO_2 fuel particles such as tri-structural isotropic or so-called TRISO-coated fuel.[1] A spherical UO_2 kernel is covered with a buffer layer, which is in turn covered with an inner high-density pyrolytic carbon (IPyC) layer. The IPyC layer is again covered with a third layer, for which SiC has been used. The 3rd layer is finally covered with an outer high-density pyrolytic carbon (OPyC) layer. The overall diameter of the TRISO-coated fuel is around 0.9 mm. The materials and roles of each coating layer are described in Table I.

The very high-temperature gas-cooled reactor (VHTR), a type of HTGR, is one of the most promising candidates for fourth generation nuclear energy systems. VHTR fuel needs to be designed with excellent safety performance up to a burn-up of about 15%–20% fissions per initial metal atom (%FIMA) and a fast neutron fluence of $6 \times 10^{25}/m^2$ (E > 0.1 MeV). The use of fuel particles such as those processed with advanced coating would improve the performance of the VHTR, as they can withstand higher temperatures and higher burn-up than existing TRISO-coated fuel particles.

In studies performed in the early 1970s and 1980s at the Japan Atomic Energy Research Institute (JAERI, forerunner of the Japan Atomic Energy Agency), zirconium carbide (ZrC)-coating conditions[2] for obtaining uniform structures and stoichiometry were successfully acquired. This was achieved by using a small-scale coating method involving only a few tens of grams per batch and a ZrC-coated fuel particle, resulting in the successful fabrication of a ZrC-coating layer. These studies demonstrated that ZrC-coated fuel particles possess much higher temperature stability than existing TRISO-coated fuel particles.[3] In addition, the ZrC-coating layer has been found to have higher resistance to Pd corrosion than a SiC-coating layer.[4]

Between 2004 and 2008, the Japan Atomic Energy Agency (JAEA) investigated the following three subjects related to the new coating layer.

1. A ZrC-coating process involving up to 200 g per batch scale with reduced excess carbon.[5–8] It should be noted that too much excess carbon adversely affects the performance of the ZrC-coating layer.[9,10]
2. Inspection methods for ZrC-coating. A method of evaluating the C/Zr ratio and ZrC density[7] has been developed for quality control of the ZrC layer.
3. The irradiation effects of ZrC-coated particles.

The authors have already reported on some characteristics of the microstructure of ZrC layers with various C/Zr ratios, including IPyC/ZrC boundary regions[11] and the effects of heat treatment on the above-mentioned characteristics.[12] It should be noted that as fuel particles are usually mixed with powder graphite, etc., before being sintered into fuel compacts, it is quite significant to study the effects of heat treatment in a way that imitates the thermal history of the sintering process.

In this study, the authors first report on the characteristics of the microstructure of ZrC layers with a C/Zr ratio of nearly 1.0, as fabricated by JAEA in the above-mentioned project, and the effects of heat treatment on those characteristics. Next, the authors report on the results of experiments in positron annihilation spectroscopy of various ZrC layers, including the above-mentioned nearly stoichiometric ZrC layers. Finally, the authors discuss problems with the quality control of ZrC layers, which were clarified with the above-mentioned characteristics of the microstructure of nearly stoichiometric ZrC layers.

Table I. Materials and the Roles of Each Coating Layer

Coating layer	Material	Role
Buffer layer	Low density pyrolytic carbon	Plenum for gases (gaseous fission products, CO gas)
Inner pyrolytic carbon (IPyC) layer	High density pyrolytic carbon	Retaining gases; Protest UO_2 kernel from material gas during deposition of the third layer
The third layer	Silicon carbide (SiC)	Main structural layer; Barrier for metallic fission products
Outer pyrolytic carbon (OPyC) layer	High density pyrolytic carbon	Cushion for the third layer

II. Experimental Procedure

(1) Fabrication of Coated Particles and Heat Treatment

(A) Fabrication of Coated Particles: Basic data on coated particles for each batch reported in this study are shown in Table II.

The samples used were ZrC-coating layers deposited at JAEA on feed particles,[11,12] except in batch H. The feed particles with a diameter of approximately 0.8 mm were spherical IPyC-coated stabilized ZrO_2 with a diameter of approximately 0.72 mm.[11,12] The surface of the feed particles was PyC, because the ZrC layer needs to be coated on PyC in a practical process for the fuel particles. The diameter of the ZrO_2 and the thickness of the IPyC layer were set to match those of particles with UO_2 kernels to be deposited with ZrC layers.[11,12] This was because the state of fluidization depends on the weight and diameter of the particles. In addition to this, UO_2 kernels are isolated from the material gas of ZrC with an IPyC layer, and as such, the state of deposition obtained is transferable to a real UO_2 system. For batch H, alumina kernels were used instead of ZrO_2 kernels to reduce radioactivity after irradiation tests with nuclear reactors.

The ZrC-coating layers were made via chemical vapor deposition (CVD) using the bromide process.[10] In the bromide process, the ZrC-coating layer is deposited through a pyrolytic reaction of zirconium bromide, CH_4 and H_2 in a fluidizing bed. The main reactions in the bromide process can be described as follows[2]:

$$[CH_4] = (C) + 2[H_2] \tag{1}$$

$$[ZrBr_4] + [H_2] \rightarrow [ZrBr_3], [ZrBr_2] + [HBr] \tag{2}$$

$$[ZrBr_x] + (C) = (ZrC) + x[Br]\,(x = 2, 3, \text{or} 4) \tag{3}$$

$$[Br] + (1/2)[H_2] = [HBr] \tag{4}$$

$$(1/4)(C) + [HBr] = (1/4)[CH_4] + [Br] \tag{5}$$
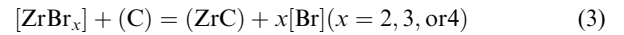
OPyC layer deposition was carried out continuously after ZrC deposition for batches F and G, via pyrolysis of propylene at about 1700 K.[6]

The deposition temperature was kept almost constant by keeping the heater power constant. However, the temperature varied by about 80 K locally in the fluidized bed.

(B) Heat Treatment: The coated particles in batches other than batch D were annealed to discover the effects of the fuel compact sintering process on microstructure evolution in the particles. The heat treatment condition was set so as to imitate the thermal history of the fuel compact sintering process for the High Temperature Engineering Test Reactor (HTTR) at JAEA. First, the coated particles were heated in a vacuum at a rate of about 200 K/min. They were then kept at around 2073 K (2033 K) for 1 h, before finally being cooled to room temperature (RT) at a cooling rate of about 140 K/min. The microstructure of the coating layer of batch A before and after heat treatment has been reported in refs. 11 and 12, respectively.

(2) Microstructural Observation

(A) Scanning Electron Microscope Observation of Fractured Coating Layers: Coated particles were mechanically crushed, and fractures in the coating layers were observed using S-3000N (Hitachi Co. Ltd, Tokyo, Japan) at RT.

(B) Transmission Electron Microscope and Scanning TEM Observation: Cross-sectional transmission electron microscope (TEM) specimens of the ZrC layers of batches F and G before and after heat treatment were prepared by a focused ion beam (FIB) micro sampling method using FB-2000A (Hitachi Co. Ltd) with 30 kV Ga ions. The preparation was made without resin embedding for the polished cross section of the particles.

TEM and scanning TEM (STEM) observations were carried out at RT using JEM-2000FX (JEOL Ltd., Tokyo, Japan) and HD-2000 (Hitachi Co. Ltd.), respectively.

(3) Positron Annihilation Spectroscopy

A positron microbeam with a diameter of 10 μm and energy of 20 keV was generated using an apparatus based on a commercial scanning electron microscope (SEM) system featuring a [22]Na source and a solid neon moderator. The details of the apparatus were as described elsewhere.[13–15] To evaluate the quality of the ZrC layers, OPyC layers were removed from

Table II. Basic Data of Each Specimen

Batch code	Batch No.	Nominal ZrC deposition temperature (K)	C/Zr ratio	Density of ZrC (g/cm³)	Note
A	ZrC-06-2003[†]	1769[12]	1.35[‡,12]	6.01[§,12]	Reported in Refs. 11 and 12
D	ZrC-06-2005[†]	1723	1.36[‡]	6.15[§]	
E	ZrC-06-2048[†]	1637	1.03[‡]	6.50[§]	
F	ZrC-07-3002	1632	1.03[‡]	6.52[§]	With OPyC layer
G	ZrC-07-3010[†]	1627	1.03[‡]	6.52[§]	With OPyC layer
H	ZrC-Al-2001[†]	1557	1.05[‡]	6.52[§]	

[†]Particles on which ZrC layer was deposited were zirconia kernel with IPyC layer[12] for batch A to G, alumina kernel with IPyC layer for batch H.
[‡]Evaluated by the infrared light absorption during combustion in oxygen and by the inductively coupled plasma-atomic emission spectrometry (ICP-AES).[8]
[§]Evaluated by the gas pycnometer method.[8]

all particle specimens. The positron microbeam was then aimed at the ZrC layers. The average implantation depth of positrons was estimated to be 0.8 μm. Doppler broadening of annihilation radiation (DBAR) measurements were carried out using a high-purity Ge detector with an energy resolution of 1.4 keV at 511 keV. DBAR spectra were characterized by S and W parameters, defined as the spectrum peak and tail area intensities, respectively. These energy windows were 510.19–511.8 and 512.28–519.52 keV. Powdered ZrC with a purity of 99% and an average particle size of 45 μm was used as a reference specimen because it exhibited the lowest S and the highest W parameters compared with the ZrC layers prepared in this study. All the S and W parameters were normalized to those obtained for the powder specimen. Generally, S and W parameters are proportional to the annihilation probabilities of positrons with valence and core electrons, respectively. Hence, the S parameter increases (W parameter decreases) when positrons are trapped at vacancy type defects due to an increase (decrease) in annihilation probability with valence (core) electrons. Thus, vacancy type defects are detected from the increase (decrease) in the S (W) parameter.

III. Results

(1) Microstructural Observation

(A) SEM Observation of Fractures in the Coating Layers: Fracture surfaces of the ZrC layers of batches E to H, with C/Zr radios of nearly 1.0 (as shown in Table II), were observed by SEM. Before heat treatment, the fracture surfaces of the ZrC layers seemed to show columnar characteris-

tics, but the outlines of the crystal grains were not clearly identified in all batches. After heat treatment, the outlines of the ZrC crystal grains were clearly identified only in batches F and H, as shown in Fig. 1. This result shows that remarkable crystal grain growth only occurred with heat treatment in batches F and H. It should especially be noted that remarkable growth in ZrC crystal grains occurred in batch F, but not in batch G, as shown in Fig. 1, in spite of both having the same C/Zr ratio and ZrC density, as shown in Table II.

(B) TEM/STEM Observation: The ZrC layers of the above-mentioned batches F and G were observed with TEM and STEM. The results of the TEM/STEM observation are summarized in Table III.

(a) Batch F: Before heat treatment: Figure 2(a) shows a STEM bright field image of the ZrC layer near the surface of the layer. The electron diffraction image in Fig. 2(a) was taken by TEM. ZrC grains were columnar in shape in the ZrC-coating layer near the surface of the ZrC layer; the average sizes of the ZrC grains were around 50–100 and 200–600 nm, oriented parallel to the circumferential and growth directions, respectively [Fig. 2(a)]. The normals of the (110) plane of ZrC grains were oriented toward the growth direction, as shown in the electron diffraction image in Fig. 2(a). Figure 2(b) shows a high-angle annular dark field (HAADF) image of the same region as Fig. 2(a). Only very few dark regions, corresponding to voids or free carbon regions,[16] were distributed in the ZrC layer, as shown in Fig. 2(b).

Figures 2(c) and (d) show TEM images of the region including the IPyC/ZrC boundary. In the vicinity of the IPyC/ZrC boundary, the ZrC grains were granular (not
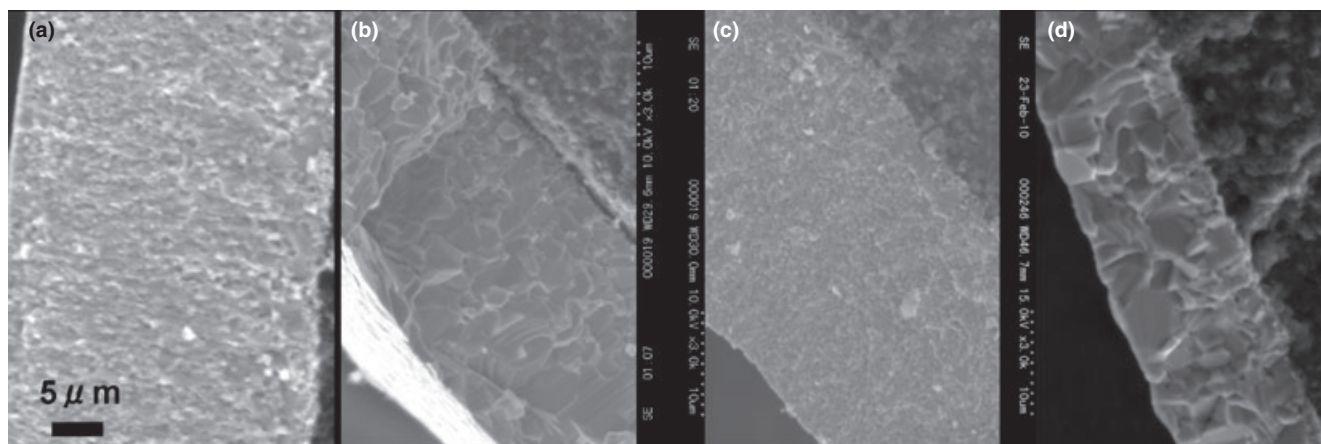
Fig. 1. SEM images of fractured coating layers after heat treatment, (a) E-batch, (b) F-batch, (c) G-batch, (d) H-batch.

Table III. Summary of TEM/STEM Observation of ZrC Layers

	Before heat treatment	After heat treatment

Batch F	*Size and shape of ZrC grains
	  –Near surface
	  Columnar (50–100 × 200–600 nm)
	  –Near IPyC/ZrC boundary
	  –granular (~100 nm)
	  –some grains were relatively large (~1 μm)
	  and granular
	*Orientation: Normals of (110)//growth direction
	  (near surface)
	*Very few voids or carbons
		*Size and shape of ZrC grains
		  –Remarkable ZrC grain growth was observed
		  max 5 μm (not columnar)
		  –relatively small (~1 μm) grains were
		  distributed in a region
		*Orientation: not clarified
		*Pores were observed on grain boundaries

Batch G	*Size and shape of ZrC grains (near surface)
	  Columnar (~100 × 250–300 nm)
	*Orientation: Normals of (200) were diffusely oriented
	  to growth direction (near surface)
	*Voids or carbons were distributed
		*Size and shape of ZrC grains: ZrC grain growth
		  was observed
		  max 1 μm (not columnar)
		*Orientation: not clarified
		*Pores were observed on grain boundaries
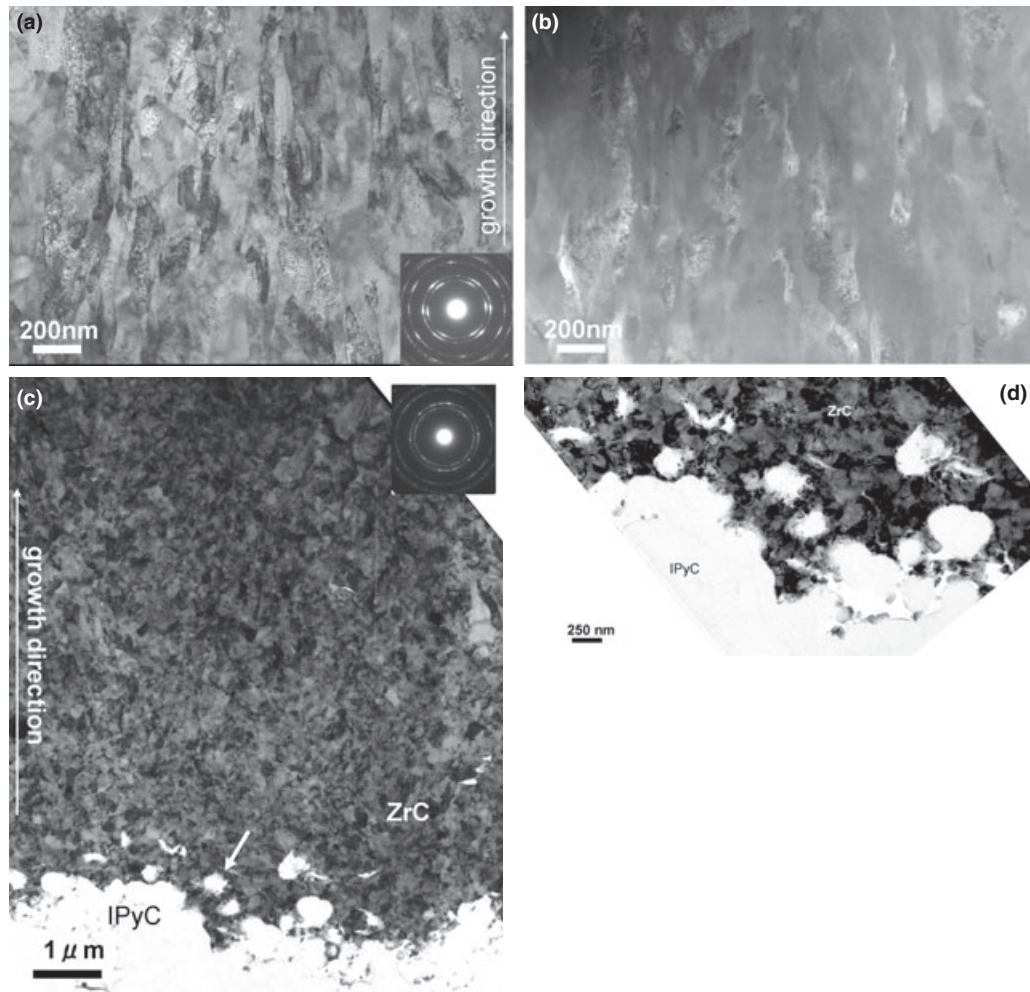
Fig. 2. TEM/STEM images of cross section of coating layer of F-batch before heat treatment, (a) STEM bright field image near surface of ZrC layer (electron diffraction image was taken with TEM), (b) HAADF image corresponding to (a), (c) TEM bright image including IPyC/ZrC boundary, (d) enlarged image near arrow in (c).

columnar) in shape and their mean size was about 100 nm. The shapes of the ZrC grains tended to be elongated in regions where the distance from the boundary was more than 3 μm. However, the preferred orientation was not clarified, as shown in the electron diffraction image in Fig. 2(c). Some grains were relatively large (about 1 μm) and granular around 5 μm from the boundary. The structure of the boundary was very similar to that of batch C,[11] of which the C/Zr ratio was 1.11. IPyC and ZrC were bound to each other, as shown in Fig. 2(d). No peculiar structure including turbostratic carbon, as observed in the case of C/Zr = 1.35 (batch A),[11] was observed in the boundary region.

After heat treatment: The region including the IPyC/ZrC boundary was observed after heat treatment, as shown in Fig. 3(a). Remarkable ZrC grain growth occurred with heat treatment, except in the vicinity of the boundary. The ZrC grains were not columnar in shape and the size of the ZrC grains was about 5 μm at most. From the SEM image of the fracture in the coating layer, it is supposed that the maximum ZrC grain sizes are larger near the surface of the ZrC layer [Fig. 1(b)]. There was also a region where relatively small (maximum 1 μm) grains were distributed near arrow b in Fig. 3(a). The preferred orientation of the ZrC grains was not clarified from the electron diffraction, because only a small number of grains were included in the TEM specimen. Pores were observed on the grain boundaries, as shown in Fig. 3(a). In addition, a carbon region was observed on the grain boundary, as shown in Fig. 3(b). It is not clear whether the carbon was part of the IPyC layer or whether the free carbon was

swept out to the grain boundary due to ZrC grain growth, as observed in the heat-treated batch A specimen.[12]

A partially detached IPyC/ZrC boundary was found, as shown in Figs. 3(a) and (c). No peculiar structure containing standing fibrous carbons, as observed in the case of C/Zr = 1.11 (batch C) after heat treatment,[12] was observed in the boundary region. The ZrC grains were around 300 nm in size and rather small on the IPyC/ZrC boundary, as shown in Fig. 3(c).

(b) Batch G: Before heat treatment: Figure 4(a) shows a STEM bright field image of the ZrC layer near the surface of the layer. The electron diffraction image in Fig. 4(a) was taken by TEM. The normals of the (200) plane of ZrC grains were diffusely oriented toward the growth direction, as shown in the electron diffraction image in Fig. 4(a). The orientations appeared similar to those observed in batch C (C/Zr = 1.11).[11] ZrC grains were columnar in shape in the ZrC-coating layer near the surface of the ZrC layer; the average sizes of the ZrC grains appeared to be around 100 nm and 250–300 nm, oriented parallel to the circumferential and growth directions, respectively, as shown in Fig. 4(a). It is difficult to estimate the length of the columnar grains unless the longitude direction of the grain and the normal of the specimen's cross section are perpendicular to each other. Nevertheless, the average length of the grains should in fact be shorter in batch G than in batch F, due to the diffuse orientation of the normals of the (200) plane.

Figure 4(b) shows a HAADF image of the same region as Fig. 4(a). The dark regions, corresponding to voids or free carbon regions,[16] were distributed in lines roughly perpendic-
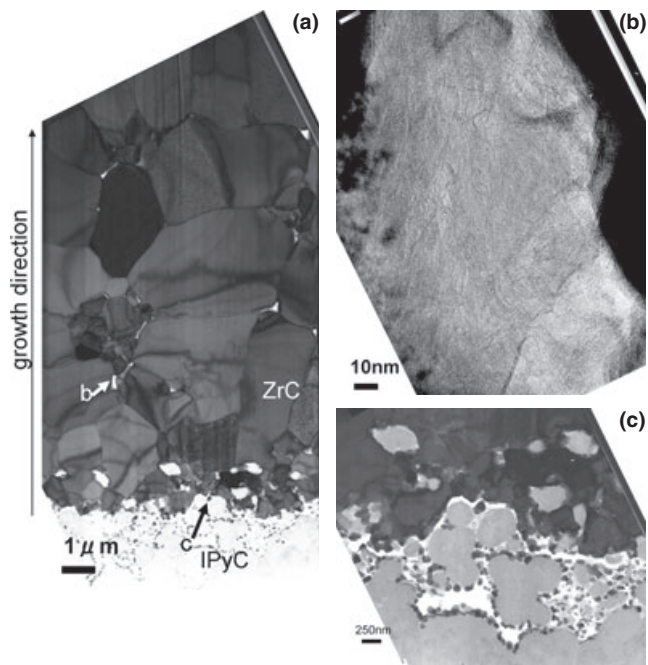
Fig. 3. TEM images of cross section of coating layer of F-batch including IPyC/ZrC boundary after heat treatment, (a) TEM bright image, (b) enlarged image near arrow b in (a), (c) enlarged image near arrow c in (a).

ular to the growth direction. It should be noted that small free carbon regions (or voids) are buried in near stoichiometric ZrC layers. Then it was impossible to distinguish free carbons and voids by confirmation of the feature of the carbon[10,11] with TEM observation as well as carbon rich with STEM/EDX in such regions.

After heat treatment: Figure 5(a) shows a HAADF image of the ZrC layer near the surface of the layer. ZrC grain growth occurred with heat treatment. Most of the ZrC grains were not columnar in shape and the size of the grains was about 1 μm at most, as shown in Fig. 5(a). ZrC layers with a smaller grain size may be inferior to those with a larger grain size in their fission product (FP) retention performance. In addition, ZrC layers in G batch would not be mechanically stronger than that in batch F in spite of the smaller grain size than that in batch F, because the grain growth with heat treatment was hindered by voids or free carbon, which is much weaker than the ZrC matrix.

The preferred orientation of the ZrC grains was not clarified from the electron diffraction. Pores were observed on the grain boundaries, as shown in Fig. 5(a). The pores were not distributed in lines roughly perpendicular to the growth direction as observed in the heat-treated batch C,[12] as shown in Fig. 5(a). A relatively large pore was found to include carbon

bons, as shown in Fig. 5(b). This carbon is probably not part of the IPyC layer because it was not near the IPyC/ZrC boundary, but derives from free carbons swept out to the ZrC grain boundary due to the growth of ZrC grains.[12]

(2) Positron Annihilation Spectroscopy

Figure 6(a) shows the S and W parameters obtained through DBAR measurements of the ZrC layers fabricated in various batches before heat treatment, as listed in Table II. The ZrC layers prepared in this study exhibited higher S and lower W parameters compared with the reference powder ZrC specimen. This indicates the presence of vacancy type defects in the ZrC layers; however, the vacancy type defects are not identified yet. There were two clearly separated groups on the S-W plane. One included batches A and D with a high C/Zr ratio (1.35), exhibiting higher S and lower W parameters. The other included batches E to H with C/Zr of around 1.0, exhibiting lower S and higher W parameters. In the latter group, moreover, batches F and H, in which remarkable ZrC grain growth was observed by SEM as shown in Fig. 1, gave rise to even lower S and higher W parameters. It is interesting to note that the S and W parameters of the ZrC layers fabricated in batches F and G were significantly different from each other even though the C/Zr ratios and the material densities for these specimens were nearly the same as shown in Table II.

Figure 6(b) shows the S and W parameters of ZrC layers fabricated in batches F and G before and after heat treatment. Upon heating, the S and W parameters changed toward the direction of the reference powder ZrC specimen, with similar amounts for batches F and G. This indicates that commonly included vacancy type defects in batches F and G were annealed out at 2033 K. Meanwhile, the differences in S and W parameters between batch F and G after heat treatment were preserved during heat treatment. This implies that vacancy type defects giving rise to a higher S (lower W) parameter of batch G were even retained at 2033 K.

IV. Discussion

Although the C/Zr ratio and density of the ZrC layers of batches E to H were similar, as shown in Table II, remarkable differences were observed in the microstructures of these layers after heat treatment, a condition set to imitate the thermal history of the fuel compact sintering process, as shown in Figs. 1(a)–(d). It should be noted that batches F and G were fabricated under similar conditions and that the C/Zr ratio and density of the ZrC layers were estimated to be the same.

TEM/STEM observation of the specimens before heat treatment clarified that many more free carbons or voids were distributed in the ZrC layer in batch G than in batch F, as shown in Figs. 2(b) and 4(b), and that the types of crystal-
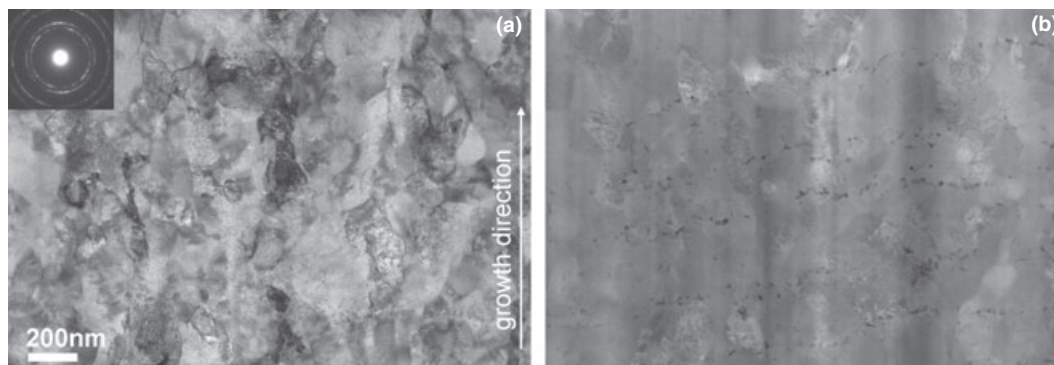
Fig. 4. TEM/STEM images of cross section of coating layer of G-batch before heat treatment, (a) STEM bright field image near surface of ZrC layer (electron diffraction image was taken with TEM), (b) HAADF image corresponding to (a).
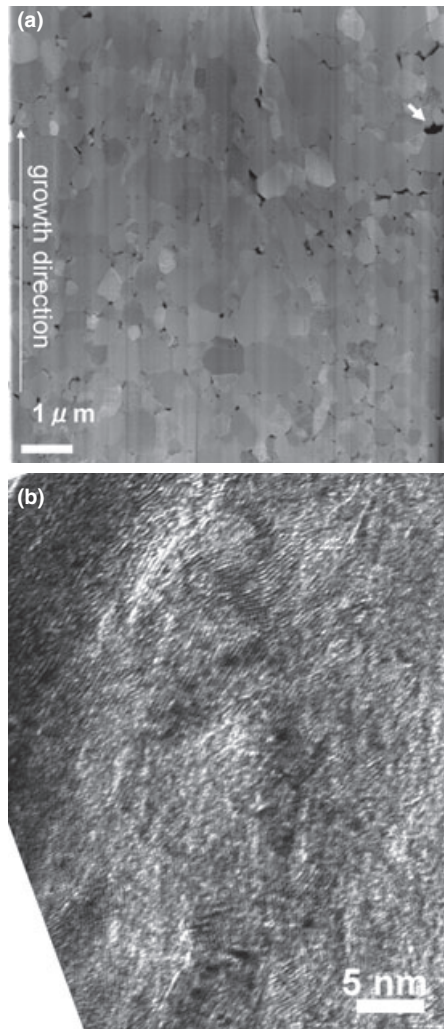
Fig. 5. TEM/STEM images of cross section of coating layer of G-batch after heat treatment, (a) HAADF image near surface of ZrC layer, (b) enlarged TEM image near arrow in (a).

lographic orientation of the ZrC grains were different in these two batches, as shown in Figs. 2(a) and 4(a). It would be reasonable to assume that the free carbons or voids hindered ZrC crystal growth with heat treatment in batch G.

The fission product retention performance and mechanical properties (especially those related to plastic deformation) of the ZrC layers appears to depend strongly on microstructure after heat treatment, including ZrC grain size. The possibility should be noted that the ZrC layer may deform plastically under irradiation.[17] Thus, the quality of the ZrC layers of the coated fuel particles must be controlled to give the microstructure of the ZrC layer desirable characteristics after the fuel compact sintering process. This makes it clear that measurements of the C/Zr ratio and ZrC density are not sufficient for quality control of the ZrC layers.

Sufficient quality control may be possible by adding TEM/STEM observation to the inspection subjects, but it is not suitable for routine inspection of practical fuel particles, owing to the difficulty in preparing specimens. SEM observation of fractured ZrC layers after heat treatment may be applied for quality control of the ZrC layers, if the ZrC grain were to grow to a size that can be estimated with SEM observation. In any case, microstructural observation is not very desirable as a subject of routine inspection of practical fuel particles, owing to the difficulty in achieving quantitative evaluation.

On the other hand, there is a clear correlation between the microstructure of ZrC layers after heat treatment and the
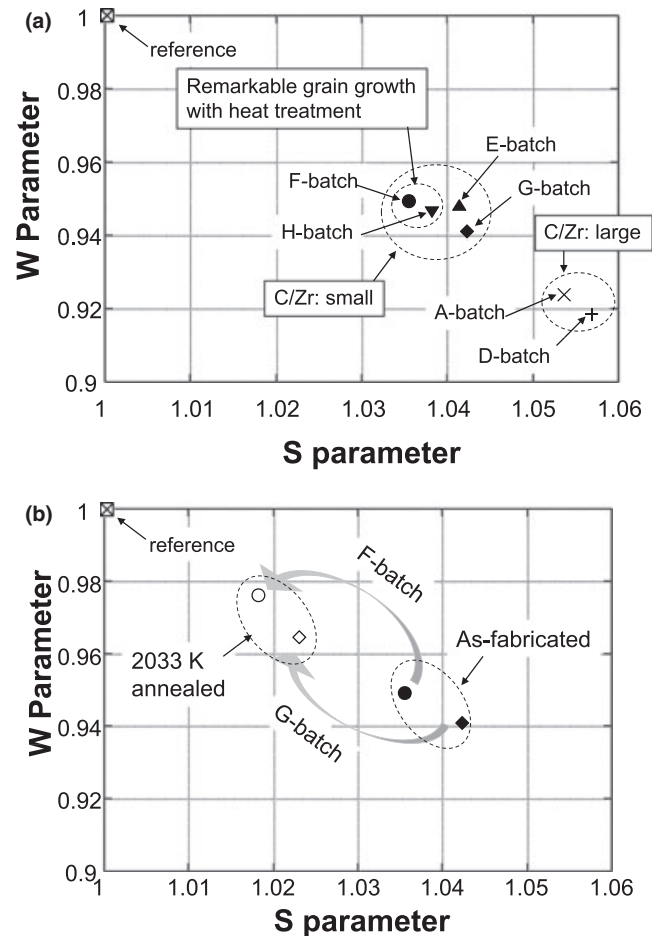
Fig. 6. S and W parameters on surface of ZrC layer, (a) various specimens before heat treatment, (b) change with heat treatment on F- and G-batches.

S and W parameters of the ZrC layers before heat treatment [Fig. 6(a)]. It should especially be noted that differences between batches F and G, which could not be detected by estimating the C/Zr ratio and ZrC density, could be detected with positron annihilation spectroscopy (PAS), as shown in Fig. 6(b). In addition, specimen preparation for PAS is much easier than that for TEM/STEM observation. Specimens for PAS measurement of the surface of ZrC layers can be prepared easily, for example, by crushing the coated particles and picking up fragments without OPyC layers. Moreover, PAS is much more suitable for quantitative evaluation than microstructural observation. Thus, PAS might be suitable as a method of quality control for ZrC-coated fuel particles.

On the other hand, the defects reflected to the S and W parameters of the ZrC layers are not identified yet, as mentioned above. Positron lifetime measurements and a comparison between DBAR and theoretical calculations would be the next step for investigation of the feasibility of the application of PAS to the quality control of ZrC-coated fuel particles.

Although it would be reasonable to assume that free carbons or voids hindered ZrC crystal growth with heat treatment in batch G, as mentioned above, the following important problems still remain.

1. Why were many more free carbons or voids distributed in the ZrC layer in batch G than in batch F, in spite of both having the same C/Zr ratio and ZrC density?
2. In addition, why did remarkable grain growth occur with heat treatment in batch H, in spite of the larger C/Zr ratio than in batch G?

These problems may be related to the fact that the ZrC phase has a large composition range in carbon-poor regions.[18]

V. Conclusions

ZrC-coated particles fabricated by JAEA, with C/Zr radios of nearly 1.0, were annealed under a condition imitating the thermal history of the fuel compact sintering process. SEM observation of fractures in the coating layers revealed that remarkable growth in ZrC crystal grains occurred with heat treatment in some batches, but not in others. It should especially be noted that remarkable growth in ZrC crystal grains occurred in batch F, but not in batch G, in spite of both having the same C/Zr ratio and ZrC density. This makes it clear that measurements of the C/Zr ratio and ZrC density are not sufficient for quality control of ZrC layers because the performance and properties of the ZrC layers must depend strongly on the microstructure after heat treatment, including the ZrC grain size. TEM/STEM observation of the specimens before heat treatment clarified that many more free carbons or voids, which would hinder ZrC crystal grain growth with heat treatment, were distributed in the ZrC layer in batch G than in batch F.

Finally, there is also a clear correlation between the microstructure of ZrC layers after heat treatment and the S and W parameters of ZrC layers before heat treatment. It should especially be noted that differences between batches F and G, which could not be detected by estimating the C/Zr ratio and ZrC density, could be detected with PAS. PAS might therefore be suitable as a method of quality control for ZrC-coated fuel particles, as preparing specimens for PAS is much easier than for TEM/STEM observation. Moreover, PAS is much more suitable for quantitative evaluation than microstructural observation. Characterizing the defects detected with PAS would be the next step for the investigation of the feasibility of the application of PAS to the quality control of ZrC-coated fuel particles.

Acknowledgments

References

[1]K. Fukuda, T. Ogawa, K. Hayashi, S. Shiozawa, H. Tsuruta, I. Tanaka, N. Suzuki, S. Yoshimuta, and M. Kaneko, "Research and Development of HTTR Coated Particle Fuel," *J. Nucl. Sci. Technol.*, **28**, 570–81 (1991).

[2]T. Ogawa, K. Ikawa, and K. Iwamoto, "Chemical Vapor Deposition of ZrC within a Spouted Bed by Bromide Process," *J. Nucl. Mater.*, **97**, 104–12 (1981).

[3]T. Ogawa, K. Fukuda, S. Kashimura, T. Tobita, F. Kobayashi, S. Kado, H. Miyanishi, I. Talahashi, and T. Kikuchi, "Performance of ZrC-Coated Particle Fuel in Irradiation and Postirradiation Heating Tests," *J. Am. Ceram. Soc.*, **75**, 2985–90 (1992).

[4]T. Ogawa and K. Ikawa, "Reaction of Pd with SiC and ZrC," *High Temp. Sci.*, **22**, 179–93 (1986).

[5]A. Yasuda, S. Ueta, J. Aihara, H. Takeuchi, and K. Sawa, "Development of Production Technology of ZrC-Coated Particle (No. 1)", JAEA-Technology 2008-073 (2008). (in Japanese)

[6]A. Yasuda, S. Ueta, J. Aihara, T. Takeuchi, and K. Sawa, "Development of Production Technology of ZrC-Coated Particle (No. 2)," *JAEA-Technology*, 2008–083 (2008). (in Japanese)

[7]S. Ueta, J. Aihara, A. Yasuda, H. Ishibashi, Y. Mozumi, K. Sawa, and K. Minato, "Development on Fabrication Techniques for the ZrC-Coated Fuel Particle as an Advanced High Temperature Gas Cooled Reactor Fuel," *Hyomen*, **46**, 222–32 (2008). (in Japanese)

[8]S. Ueta, J. Aihara, A. Yasuda, H. Ishibashi, T. Takayama, and K. Sawa, "Fablication of Uniform ZrC Coating Layer for the Coated Fuel Particle of the Very High Temperature Reactor," *J. Nucl. Mater.*, **376**, 146–51 (2008).

[9]K. Minato and T. Ogawa, "Research and Development of ZrC-Coated Particle Fuel"; pp. 1068–74 *Proc. GLOBAL*, New Orleans, LA, USA, 2003.

[10]T. Ogawa, K. Ikawa, and K. Iwamoto, "Microhardness and Microstructure of Chemically Vapor Deposited ZrC-C Alloy," *J. Nucl. Mater.*, **62**, 322–4 (1976).

[11]J. Aihara, S. Ueta, A. Yasuda, H. Ishibashi, Y. Mozumi, K. Sawa, and Y. Motohashi, "TEM/STEM Observation of ZrC Coating Layer for Advanced High-Temperature Gas-Cooled Reactor Fuel, Part II," *J. Am. Ceram. Soc.*, **92**, 197–203 (2009).

[12]J. Aihara, S. Ueta, A. Yasuda, H. Takeuchi, Y. Mozumi, K. Sawa, and Y. Motohashi, "Effect of Heat Treatment on TEM Microstructures of Zirconium Carbide Layer in Fuel Particle for Advanced High Temperature Gas Cooled Reactor," *Mater. Trans.*, **50**, 2631–6 (2009).

[13]M. Maekawa and A. Kawasuso, "Construction of a Positron Microbeam in JAEA," *Appl. Surf. Sci.*, **255**, 39–41 (2008).

[14]M. Maekawa, A. Kawasuso, T. Hirade, and Y. Miwa, "Application of Positron Microprobe for Nuclear Materials," *Mater. Sci. Forum*, **607**, 266–8 (2009).

[15]M. Maekawa, A. Kawasuso, T. Hirade, and Y. Miwa, "Development and Application of Positron Microprobe," *Trans. Mater. Res. Soc. Jap.*, **33**, 334–7 (2008).

[16]J. Aihara, S. Ueta, A. Yasuda, H. Ishibashi, T. Takayama, K. Sawa, and Y. Motohashi, "TEM/STEM Observation of ZrC-Coating Layer for Advanced High-Temperature Gas-Cooled Reactor Fuel," *J. Am. Ceram. Soc.*, **90**, 3968–72 (2007).

[17]T. Ogawa, K. Ikawa, K. Fukuda, S. Kashimura, and I. Iwamoto, "Research and Development of ZrC-Coated UO2 Particle Fuel at the Japan Atomic Energy Research Institute", pp. 163–9 *Proc. BNES Conf. Nuclear Fuel Performance*, 1985.

[18]A. F. Guillermet, "Analysis of Thermochemical Properties and Phase Stability in the Zirconium-Carbon System," *J. Alloys Compd.*, **21**, 69–89 (1995). □